Broadband Analysis of a D-Band Holographic Power Combining Circuit

M. Höft[1], J. Weinzierl[2], and R. Judaschke[1]

[1] Technische Universität Hamburg-Harburg
Arbeitsbereich Hochfrequenztechnik
D-21071 Hamburg, Germany

[2] Universität Erlangen-Nürnberg
Lehrstuhl für Hochfrequenztechnik
D-91058 Erlangen, Germany

Abstract – Holography is a promising technique for power combining applications in the frequency range of short millimeter and submillimeter waves. In this paper, a quasi-optical holographic power combining circuit is investigated. The hologram is designed for 150 GHz and has an efficiency of 92.5 % with a 90 % bandwidth of 5.3 %. With help of a broadband waveguide power splitter and a vector field measurement system, the circuit is analyzed.

I. Holographic Power Combining

Highly efficient solid-state power combining in the frequency range of short millimeter and submillimeter waves should be performed in free-space to avoid ohmic losses [1]. Consequently, the individual sources have to be placed in an array. On the other hand, there is a general restriction concerning the limitation of the inter-element spacing due to thermal demands, single-device housing geometry, and beam launcher aperture. Therefore, this distance is restricted to several wavelengths. Hence, grating lobes occur in the radiation pattern, and the combining efficiency decreases drastically.

To overcome this problem, holography can be utilized [2]. The hologram stores the interference pattern of both the input waves and the desired output beam, so that the latter will be reconstructed if the hologram is illuminated by the input waves. The experimental setup is depicted in the lower part of Fig. 1 for five single-element sources with distance L. The hologram which is located in the near-field of the horn array consists of a dielectric surface-relief grating with relative permittivity ε_r.

If the number of devices is large enough, the hologram can be designed as a periodic structure with the same periodicity length L. In this case, the optimization of the structure can be performed by assuming both parts – horns and hologram – to be periodically extended to infinity. Due to this, the free-space propagation can be described by a denumerable set of space harmonics. In the upper part of Fig. 1, the space harmonics (plane waves) above cut-off

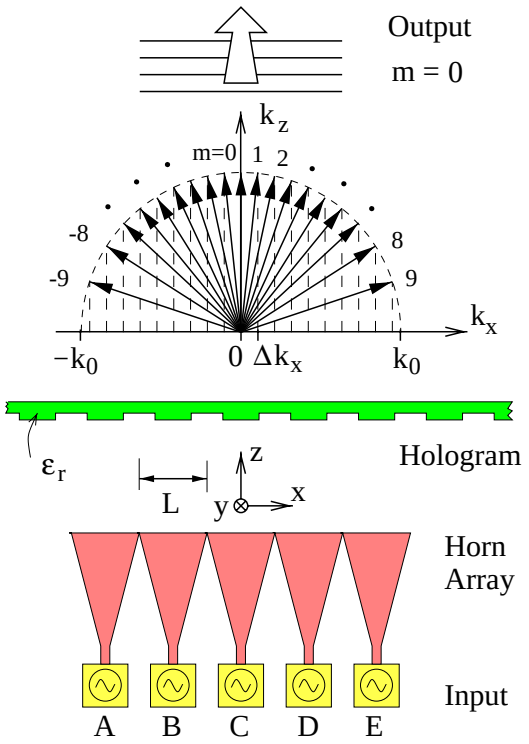

Fig. 1: Setup of the holographic power combining circuit. In the upper part, the space harmonics above cut-off for L/λ = 9.5 are depicted.

are sketched for L = 19 mm, f = 150 GHz. Note that these modes correspond to the resulting grating lobes for the finite case.

The optimization of the power combining circuit can be performed by modeling the structure by an equivalent network as described in [2]. A well designed hologram maximizes the power which is combined in the perpendicular plane wave, i.e. m = 0 (Fig. 1). This leads to a pseudo-plane wave for the finite array. It should be noted that it is advantageous to include the horn antenna geometry into the design procedure for a higher degree of freedom to find the optimum efficiency of the circuit.

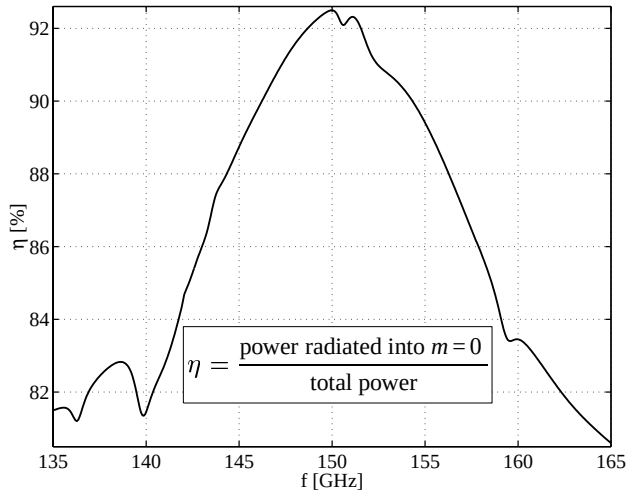

Fig. 2: Calculated combining efficiency of the hologram.

II. Broadband behavior

A hologram for a center frequency of 150 GHz has been designed consisting of a simple rectangular groove shape for the periodic structure. The hologram consists of Teflon (ε_r = 2,06). The grooves have a depth of 1.39 mm, a width of 5.87 mm, and are placed on a slab with a thickness of 2.08 mm. The hologram is located at a distance of 28.1 mm in front of the horn antennas which have an aperture width of 17.6 mm and a horn length of 33.0 mm. The resulting power combining efficiency for the infinite array has been calculated to be 92.5 %.

The frequency dependence of the efficiency is shown in Fig. 2. Assuming a tolerable efficiency of 90 % leads to a bandwidth of 8 GHz or 5.3 %, respectively.

Note, that this simple type of hologram is chosen due to manufacturing considerations. The efficiency could be increased by introducing a more complex surface. It should be noted that our inter-element spacing of $L/\lambda = 9$ limits the performance, since efficiencies up to 99 % with a bandwidth larger than 11 % can be achieved with rectangular groove shapes for lower spacings ($L/\lambda < 7.5$) [1].

III. Measurement techniques

Vector near-field measurements can been performed in the plane where the hologram should be located to verify the calculated field distributions of the horn antenna array. In addition, these information can be directly used as input data for the hologram design, e.g. for arbitrary antenna arrays.

To prove the performance of the power combining circuit, the field distribution can be measured in a distance of some wavelengths behind the hologram. Under operation with free running oscillators synchronization and coherent, in-phase oscillation can be investigated. In a first step, measurements have been performed with a broadband power splitter for equal excitation of the single antennas to characterize the hologram independently of the behavior of the active sources.

A. Broadband power splitter

Since efficiency is of lower importance for the splitter, it is designed as a symmetrical four-stage coupler-waveguide-network (Fig. 3). In principle, there are six output ports of equal transmission, i.e. the input signal twice passes along both the through- and coupling-path (S_{21} and S_{31}, resp.) of a single coupler. However, only five of them are used. Under the assumption of matched ports ($S_{ii} = 0$), ideal directivity (S_{41} = 0 and S_{23} = 0), and identical directional couplers for all stages, the resulting output signal equals $E_{out} \propto {S_{21}}^2 \cdot {S_{31}}^2 \cdot E_{in}$ for all five ports. The waveguides were chosen to be equal in length to obtain identical phases for these ports. The remaining ports have been terminated with matched loads.

With this concept, all output signals are identical with respect to magnitude and phase independently of the single coupler frequency behavior (S_{21} and S_{31}) as long as the coupler input reflection stays reasonably low and the isolation high.

We applied ridge-shaped narrow-wall directional couplers [3] due to their simple structure. They are suitable even at short millimeter-wavelengths, since the coupling region consists of a ridge waveguide where the ridge width is defined by the waveguide spacing. The coupling behavior is determined by ridge width, ridge height, and coupling length. For 3 dB-coupling at 150 GHz, the ridge has a width of 0.422 mm, a height of 0.640 mm, and a coupling length of 8.6 mm, respectively.

Fig. 4 shows the measured output power variation with respect to the average value of all five ports of the power

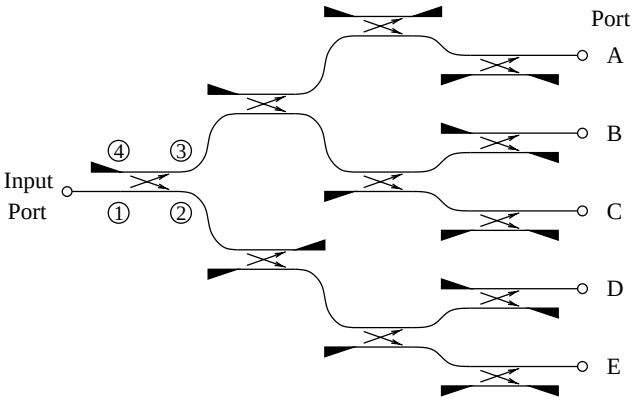

Fig. 3: Design of a broadband power splitter for measurement applications.

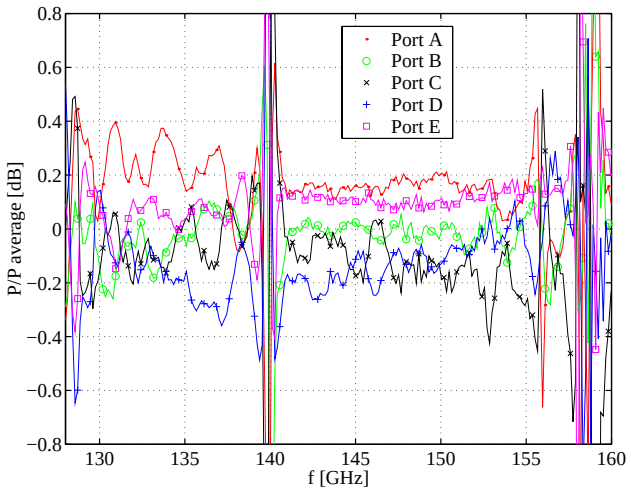

Fig. 4: Measured deviation of the output power.

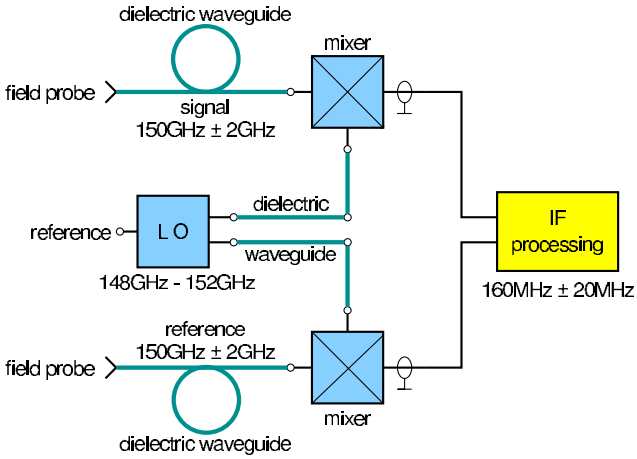

Fig. 5: General setup of the vector field measurement system.

splitter. The power variation is lower than ± 0.25 dB within a bandwidth of 10 GHz. The average overall insertion loss is 14.2 dB which corresponds to ohmic losses of 2.2 dB.

B. Vector field measurement system

The measurement of the output pattern of the horn antenna array in both cases – with and without hologram – was performed by a vector field measurement system which was designed to operate in the frequency range from 148 to 152 GHz with a dynamic range of 75 dB and a phase uncertainty lower than 3 degree. The general setup of the system is shown in Fig. 5 [4]. It uses two receiver channels, a signal channel mounted on a 3D scanning platform, and a spatially fixed reference channel, which is necessary for relative phase measurements. Fundamental balanced mixers are installed in both receiver channels.

Due to the relative movement between the signal and the reference channel during field scanning, the RF-signal is fed to the mixer via a flexible dielectric waveguide system based on dielectric fibres of rectangular cross section made of polyethylene. To minimize the field distortions of the measurement system, dielectric antennas as field probes which are formed by tapered fibre ends have been used.

IV. Results

Figs. 6-9 show a comparison of measurements at 150 GHz and corresponding calculations of magnitude and phase of the electric field. The scanned plane is located in a distance of 80 mm in front of the horn array. All results indicate excellent agreement.

The electric fields of the horn array *without* hologram are depicted in Figs. 6 and 7. Due to the grating lobes, the field distribution is split in many parts with non-uniform phase and magnitude. Figs. 8 and 9 show the fields of the horn array *with* hologram. It is obvious that the hologram has reconstructed the field distribution of a line-source.

Similar comparisons have been performed at 145 GHz, again with good agreement. This confirms the validity of the predicted broadband behavior.

V. Conclusions

A quasi-optical holographic power combining circuit which was fed by a broadband power splitter has been analyzed with help of a vector field measurement system. The dielectric hologram has been designed for 150 GHz. Theoretically, it has a maximum efficiency of 92.5 % and a 90 % bandwidth of 5.3 %. Measurements and corresponding calculations show excellent agreement.

Acknowledgement

The authors would like to thank the Deutsche Forschungsgemeinschaft (DFG) for financial support.

References

[1] K. Schünemann, M. Shahabadi, R. Judaschke, "Multiple-device circuit technology for submillimeter-wave frequencies," *Proc. SPIE*, Denver, Colorado, vol. 3795, pp. 206–216, July 1999.

[2] M. Shahabadi, K. Schünemann, "Millimeter-wave holographic power splitting/combining," *IEEE Trans. Microwave Theory Tech.*, vol. MTT-45, pp. 2316–2323, Dec. 1997.

[3] T. Tanaka, "Ridge-shaped narrow wall directional coupler using TE_{10}, TE_{20}, and TE_{30} modes," *IEEE Trans. Microwave Theory Tech.*, vol. MTT-28, pp. 239–245, 1980.

[4] J. Weinzierl, R. Schulz, H. Brand, L.-P. Schmidt, "A vector field measurement system for 150 GHz," *25th Int. Conf. on Infrared and Millimeter Waves*, Beijing, China, pp. 353–354 Sept. 2000.

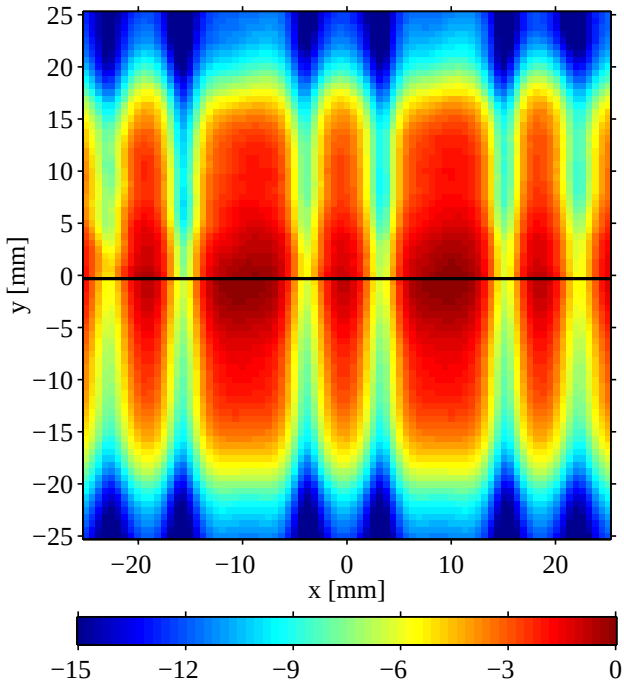

Fig. 6: Magnitude of the electric field of the horn array without hologram (scale in dB). Comparison between measurements ($y > 0$) and calculations ($y < 0$).

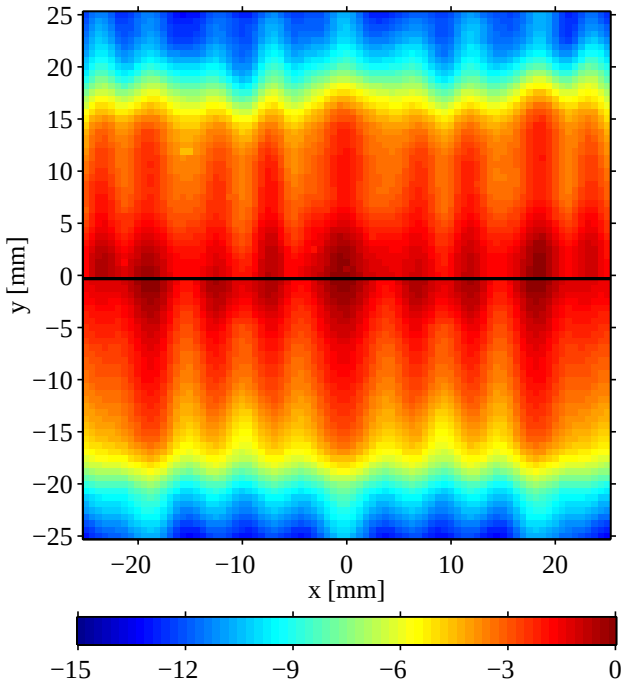

Fig. 8: Magnitude of the electric field of the horn array with hologram (scale in dB). Comparison between measurements ($y > 0$) and calculations ($y < 0$).

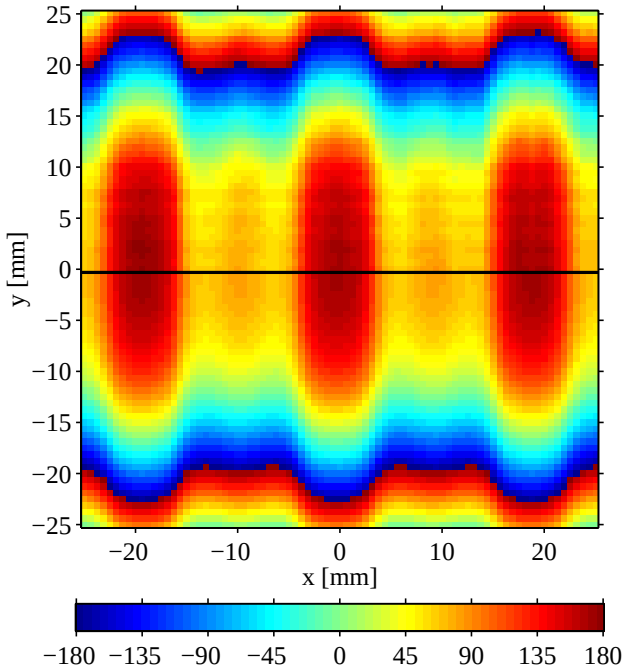

Fig. 7: Phase of the electric field of the horn array without hologram (scale in degree). Comparison between measurements ($y > 0$) and calculations ($y < 0$).

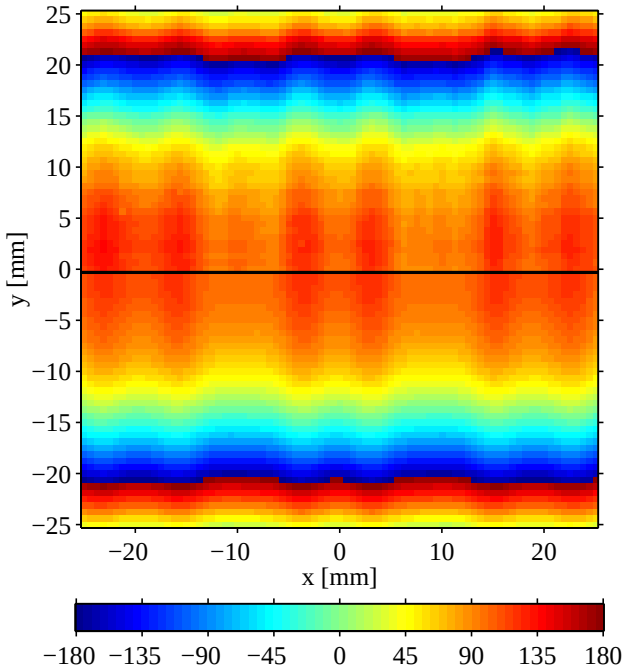

Fig. 9: Phase of the electric field of the horn array with hologram (scale in degree). Comparison between measurements ($y > 0$) and calculations ($y < 0$).